IN-VIVO TESTING OF THE BIMODAL SCAFFOLDS IN A RABBIT MODEL

Ulpan Nurmanova, Bachelor of Science

Submitted in fulfillment of the requirements for the degree of Master of Science in Biomedical Engineering

School of Engineering and Digital Sciences

Department of Chemical and Materials Engineering

Nazarbayev University

53 Kabanbay Batyr Avenue,

Nur-Sultan, Kazakhstan, 010000

Supervisors:

Lead Supervisor Name: Associate Professor Cevat Erisken

Co-supervisor Name: Assistant Professor Dana Akilbekova

April 2023

Declaration

I hereby declare that this manuscript, entitled “In-vivo testing of the bimodal scaffolds in a rabbit model” is the result of my work except for quotations and citations which have been duly acknowledged.

I also declare that, to the best of my knowledge and belief, it has not been previously or concurrently submitted, in whole or in part, for any other degree or diploma at Nazarbayev University or any other national or international institution.

Name: Ulpan Nurmanova

Date: 07.04.2023

Acknowledgements

I sincerely appreciate the opportunity to express my gratitude to all those who played a significant role in the successful accomplishment of this study. Foremost, I would like to extend my deepest thanks to my advisor, Professor Cevat Erisken, for his unwavering patience, encouragement, and invaluable suggestions that guided me throughout the entire process of organizing, conducting, progressing, and editing this research. His expertise and mentorship have been instrumental in shaping the outcome of this study. I would also like to express my heartfelt appreciation to my co-supervisor, Dr. Dana Akilbekova, for her unwavering support and guidance. Her insights and inputs have been immensely valuable in enriching the quality of this research. Furthermore, I would like to extend my gratitude to my colleagues at the Biomaterials and Interface Regenerative Engineering Laboratory for their assistance and support during the experimental tests. Their words of motivation, evaluation, and feedback have been instrumental in achieving the successful completion of this project. I am deeply grateful to everyone who has contributed to this research endeavor, and their support has been invaluable in making this study a reality. Thank you all for your unwavering encouragement, guidance, and assistance throughout this journey.

Table of Contents

List of abbreviations

ACL	Anterior Cruciate Ligament
DCM	Dichloromethane
TFA	Trifluoroacetic acid
FOV	Field of View
PET	Polyethylene terephthalate
PCL	Polycaprolactone
CFDD	Collagen fibril diameter distribution
SEM	Scanning Electron Microscopy
FA	Formic Acid
ANOVA	Analysis of Variance
AA	Acetic Acid

List of Figures and Tables

Abstract

Femur and tibia in the human body are connected by the Anterior Cruciate Ligament (ACL), which has limited capacity to self-regenerate due to low level of vascularity. Very few success rates in the clinical procedures to restore the tissue evidence that currently available clinical treatments are not optimal. Therefore, biologically similar, i.e., biomimetic, constructs that resemble healthy native tissue in their function, composition, and structure can be used to provide alternate solutions.

The hypothesis of the research is that the graft created from the alignment of Polyethylene terephthalate and Polycaprolactone (PET&PCL) nanofibers with the diameter distribution in a bimodal manner will resemble the healthy rabbit ACL's collagen fibril diameter distribution (CFDD). Histocompatibility of the ligament and bone growth would be enhanced via the biodegradable portion of the PCL, whereas the non-biodegradable PET portion would retain the integrity to prevent the deterioration of the graft's mechanical strength. To evaluate this, PET&PCL grafts were synthesized via electrospinning as a first step. Then, the alignment of the nanofibers and their fiber diameter were assessed and put into comparison with native rabbit ACL. As a third step, the mechanical quality of the synthesized grafts was evaluated and compared to the native rabbit ACL. As a final step, PET&PCL grafts were assessed in the rabbit ACL reconstruction model. PET&PCL electrospun graft's fiber diameter distribution was found to resemble the CFDD of ACL from the healthy rabbits. Also, stiffness and modulus were found to be similar.

The novelty of the study is that the nanofiber grafts from PET and PCL resembling CFDD of ACL tissue harvested in healthy rabbits were presented for the first time. This study is significant because the graft designed and fabricated here has the potential to address the needs of millions of patients suffering from ACL tears and ruptures. The design of the fibrous graft in

this study diverges from the well-known unimodal structure, and this design is expected to greatly affect ACL regeneration attempts.

Keywords: Ligament, ACL, PCL, Scanning Electron Microscope, MicroCT, Polyethylene terephthalate, Polycaprolactone, Electrospun, Nanofiber, scaffolds.

CHAPTER 1- (INTRODUCTION)

1.1 Anterior cruciate ligament tears and current treatment methods

The Anterior Cruciate Ligament (ACL), one of the two cruciate ligaments in the knee, plays a significant role in maintaining knee joint stability by preventing the tibia from sliding in relation to the femur. Unlike the other six ligaments in the knee joint, the ACL is more susceptible to injuries [1] because it often tears up when the knee is bent and the tibia rotates laterally at the same time, which requires fast turning movements while running [2]. Previous reports [3] demonstrated that approximately 69 people per 100,000 experience an ACL injury, which is more common in males than in women, and the average age for the peak of incidence is reported to be between 19-25 years. Reports also show that ligament rupture is more frequently seen in young athletic people, which requires rapid recovery and long-lasting total healing [4]. Moreover, if left untreated, the rupture of the ACL may lead to the knee joint instability, which in turn can cause dislocation or damage to other ligaments and inflammation [5]. It can also affect the menisci which can ultimately lead to osteoarthritis [6].

Because ACL tissue cannot heal itself due to its low vascularity, surgical intervention is needed to restore the function of the knee [7]. The state-of-the-art approach for ACL reconstruction is the surgical reconstruction of autografts, allografts, or synthetic grafts. Although autografts are widely regarded as the gold standard for ACL replacement, there are a number of disadvantages including increased recovery time, donor site morbidity, and a limited range of movements [8].

Since the traditional methods used in ACL replacement have a number of disadvantages, more attention is being paid to the possibilities of bioengineered grafts. In this regard, tissue engineering offers a regenerative approach for ACL injuries through the use of biomaterials,

which can be processed to incorporate some of the structural properties of the native ACL tissue into the graft.

In this thesis work, a method for the fabrication of biomimetic graft is proposed and the structural and mechanical properties of the graft were compared with those of the native ACL tissue harvested from rabbits. To prove the concept, the biomimetic graft was implanted into the anatomical position of a rabbit (n=1) and the outcomes were observed in a short term study.

1.2 Biomaterial selection and method of graft fabrication

Biomaterials are one of the essential components of regenerative engineering approach and should possess appropriate chemical and physical properties. Briefly, they should be degradable and degradation products need to be biologically compatible. Additionally, they are expected to be similar to the native ACL structurally and functionally and possibly outperform the outcomes of autografts and allografts [9]. In this study, we aimed to use a mixture of PCL and polyethylene terephthalate (PET) to fabricate synthetic ACL grafts. According to published research, synthetic polymer PCL is one of the most often utilized biomaterials for ligament replacement because of its durability and elasticity [10]. One of the reported studies [11] claimed that PCL is an appropriate material for use in regenerative medicine due to its biodegradable, biocompatible, and bioresorbable nature. Additionally, compared to other biodegradable polymers, it has appropriate viscoelastic characteristics and it is simple to create and modify a wide variety of shapes including nanofibers [12]. Furthermore, degradation products of PCL are not cytotoxic [14]. Despite these advantages of PCL, our previous reports [28] demonstrated using a rabbit ACL reconstruction model that it is unable to stabilize the knee joint due to its inferior mechanical properties in terms of both strain and resistance to loads. This behavior of PCL grafts motivated us to investigate alternative biomaterials that would stabilize the knee joint upon implantation.

In this regard, a non-degradable polymer, PET, was selected and combined with PCL to enhance the load resistance and strain of the synthetic ACL graft. Because PET is used in manufacturing the prosthetic devices due to its high tensile strength, [15], it appears as a plausible candidate for the material of fabrication of ACL grafts. As for the application of PET in orthopedic devices, it is used in the fabrication of a Ligament Advanced Reinforcement System (LARS), a synthetic ligament recommended for certain specific cases of ligament injuries [16]. Therefore, a mixture of PET&PCL graft was proposed in this study. In terms of structural similarity of the PET&PCL graft to the native ACL, the graft was designed to exhibit a bimodal fiber diameter distribution (a diameter distribution with two peaks).

Since the native ACL is formed by the collagen fibrils in the range 10nm to 400nm [25], the method of electrospinning was selected to fabricate the grafts. Electrospinning is a versatile technique for producing fibrous structures with diameters ranging from a few nanometers to a few microns, when compared to other methods developed for creating fibrous structures [18]. Moreover, by modifying the electrospinning parameters, nanofibers with diverse physical and mechanical properties can be produced [19]. These advantages make electrospinning a preferred technique for manufacturing synthetic ligament grafts.

1.3 Selection of animal model

The anatomical and physiological characteristics of animals serve as effective models for the design, testing and manufacturing of various biomedical devices. Animal models based on rabbits are widely exploited for knee joints, especially for ACL, due to the similarity in physiology and cost-effectiveness [20]. As the main objective of animal studies is to test the product in a setting that is physiologically similar to that of the human patients, anatomical similarity between the animal model and the human is an important factor to consider. A study [21] investigated the level of similarity and discrepancy of the construction and functions of the knee of humans with lapin and 5 more different animal types –bovine, ovine, caprine, porcine and canine. Although there were some differences, a significant resemblance was detected during the one-by-one assessment. The study [21] suggests that the rabbit ACL is significantly shorter and much more narrow than its human counterpart. The width and the length can be normalized using tibial plateau width to achieve similar dimensions. Moreover, according to

another published study [22], even though there is no general standard, rabbit ACL is one of the most frequently used large animal models for ACL studies. For these reasons, rabbit was used as animal model for ACL replacement.

1.4 Problem statement, study hypothesis and aims

Once injured (torn or ruptured), the ACL exhibits limited self-healing capacity due to its poor vascularity and dynamic nature. Currently available approach (gold standard) to treat ACL injuries is the reconstruction procedure using allografts; however, this option is available at the expense of increased morbidity at the donor site, reduced kinematic range, an increased risk of re-rupture, and the possibility of infection. Therefore, a more sustainable approach is needed for the healing of injured ACL. Tissue engineering offers a regenerative approach for ACL injuries through the use of biomaterials, which can be processed to incorporate some of the structural properties of the native ACL tissue into the scaffold/graft. We hypothesized that a graft fabricated from aligned PET and PCL nanofibers with bimodal diameter distribution will mimic the range of diameters of collagen fibrils in the anterior cruciate ligament of rabbits. We also hypothesize that the mechanical properties of the PET&PCL graft will be comparable to those of the natural ACL tissue, and its mechanical performance will be retained or improved after its reconstruction into rabbits. Histocompatibility of the ligament and the ingrowth of new bone would be enhanced via the biodegradable component of the ligament PCL, whereas the non-biodegradable PET portion would retain the biomechanical quality of the ACL grafts throughout its life.

The aim of this study is two folds: to design a synthetic PET&PCL graft that will imitate the distribution and organization of collagen fibers seen in normal rabbit ACL tissue using electrospinning processes and test the performance of the grafts in a rabbit ACL reconstruction model. Our objectives:

i. To fabricate PCL&PET graft by using electrospinning,

ii. To evaluate fiber diameter distribution and alignment of nanofibers and compare with native rabbit ACL,

iii. To test the mechanical properties of fabricated grafts and compare them with native rabbit ACL

iv. To test the performance of the PET&PCL graft in a rabbit ACL reconstruction model

CHAPTER 2 - (MATERIALS AND METHODS)

This chapter gives the details about: i) fabrication of nanofiber based membranes with an electrospinning device, ii) SEM characterization of membranes, iii) determination of diameter distribution of fibers and their organization, iv) fabricating grafts and performing tensile tests, v) testing the graft in a rabbit animal model, and vi) micro-CT and biomechanical characterization of the implanted graft. Figure 1 below illustrates the study approach.

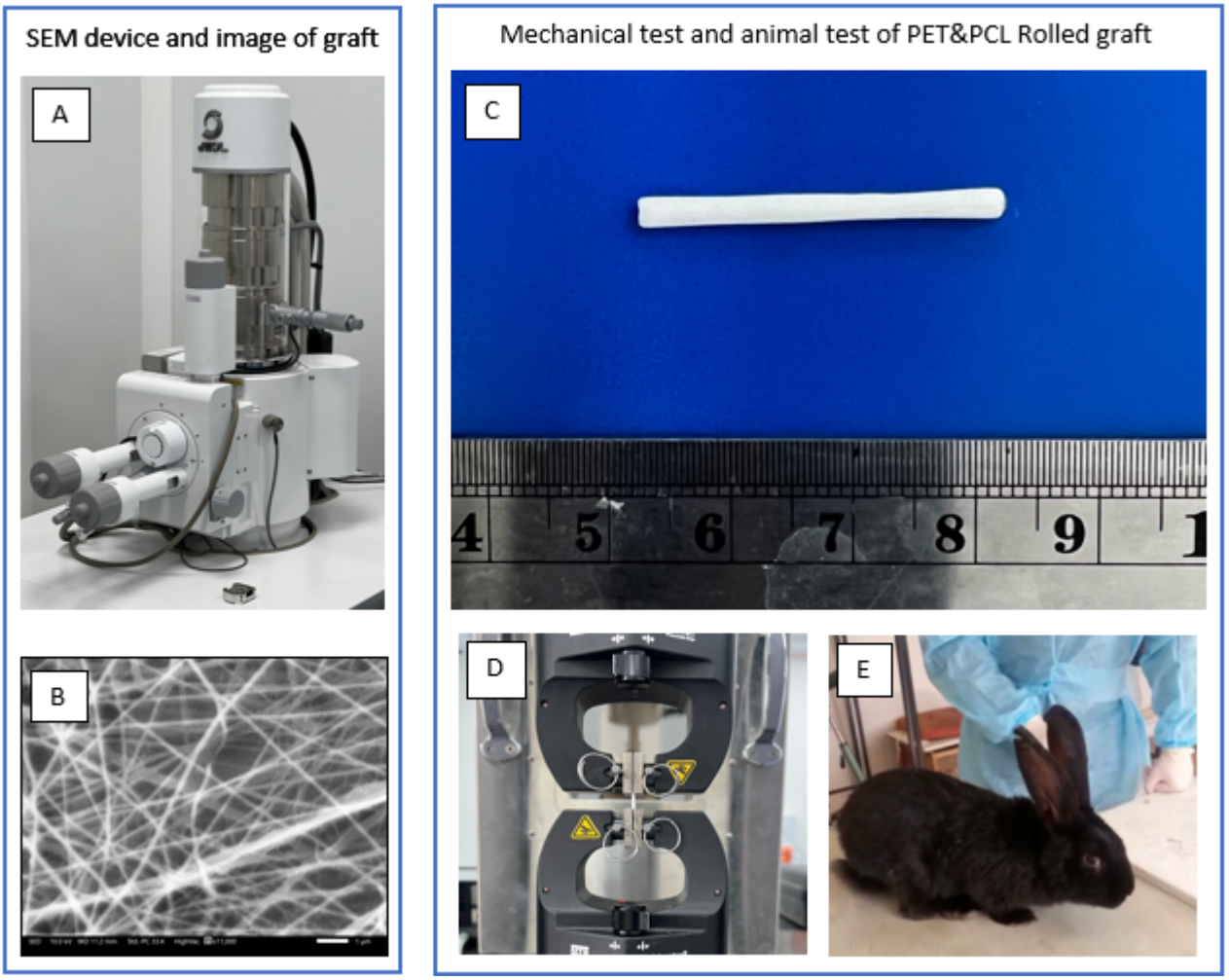

Figure 1: Representation of the experimental work

2.1 Materials

All materials except PET were obtained from Sigma Aldrich, and the product numbers are given below.

Dichloromethane (Sigma Aldrich, #270997), Polycaprolactone (Sigma-Aldrich, ##440744), formic acid (90%, #110854), Trifluoroacetic acid (Sigma Aldrich, #302031), acetic acid (#270725), pyridine (Sigma-Aldrich #270970), Polyethylene terephthalate (Coca Cola bottles - 25% recycled and 75% virgin PET).

2.2 Fabrication of nanofiber based membranes with an electrospinning device

The bimodal distribution of PET&PCL fibers were produced using PET solutions prepared in trifluoroacetic acid (TFA) and dichloromethane (DCM) while PCL solutions prepared in acetic acid (AA), formic acid (FA), and pyridine as shown in Table 1. The PET solution was performed by stirring the ingredients at 1500rpm at room temperature for 4 hours. The PCL solution was prepared by stirring the ingredients at 1500rpm and 40℃ for 2 hours.

To produce PET&PCL aligned nanofibers, a co-electrospinning method was used (Figure 2). PET and PCL concentrations of 7.5% and 8% were used, respectively. The PET solutions were transferred from two syringes to the center of a rotating drum, whereas PCL solution mounted on oppositely positioned syringe pump with one syringe. The distance from the drum to the needles tip were set to 15cm for PET and 7cm for PCL. The applied voltages were adjusted to 16 kV and 9kV for the PET and PCL solutions, respectively. The speeds of the pumping were 0.06ml/h for PET and 0.03ml/h for PCL. The drum rotated at 2000 rpm (Table 1).

The aligned bimodal PCL grafts were made from 8% and 15% concentration of PCL with 0.03 ml/h and 0.15 ml/h flow rate, 9kV and 16kV voltage, respectively (Table 2). The syringes filled with the solutions were positioned oppositely with direction to rotator drum, and distance between the needle tips and rotator was 7 cm for both of them.

Graft Type	Material Properties	Process Parameters

Bimodal PET&PCL rolled grafts		TFA (ml)	DCM (ml)	AA (ml)	FA (ml)	Pyridine (ml)	Flow rate (ml/h)	Distance (cm)	Drum Speed (rpm)	Needle Diameter (G)	Voltage (kV)
PET 7.5%	0.075 gr	0.2	0.8				0.06	15	2000	21	16
PCL 8%	0.08 gr			0.5	0.5	0.006	0.03	7	2000	21	9

Table 1: Solution formulation to create PET&PCL bimodal grafts

Graft Type		**Material Properties**				**Process Parameters**				
		PCL (gr)	Acetic Acid (ml)	Formic Acid (ml)	Pyridine (ml)	Flow rate (ml/h)	Distance (cm)	Drum Speed (RPM)	Needle Diameter (G)	Voltage (kV)
Bimodal PCL rolled grafts	8%	0.08	0.5	0.5	0.006	0.03	7	2000	21	9
	15%	0.15	0.5	0.5	0.006	0.15	7	2000	21	16

Table 2: Solution formulation to create PCL bimodal grafts

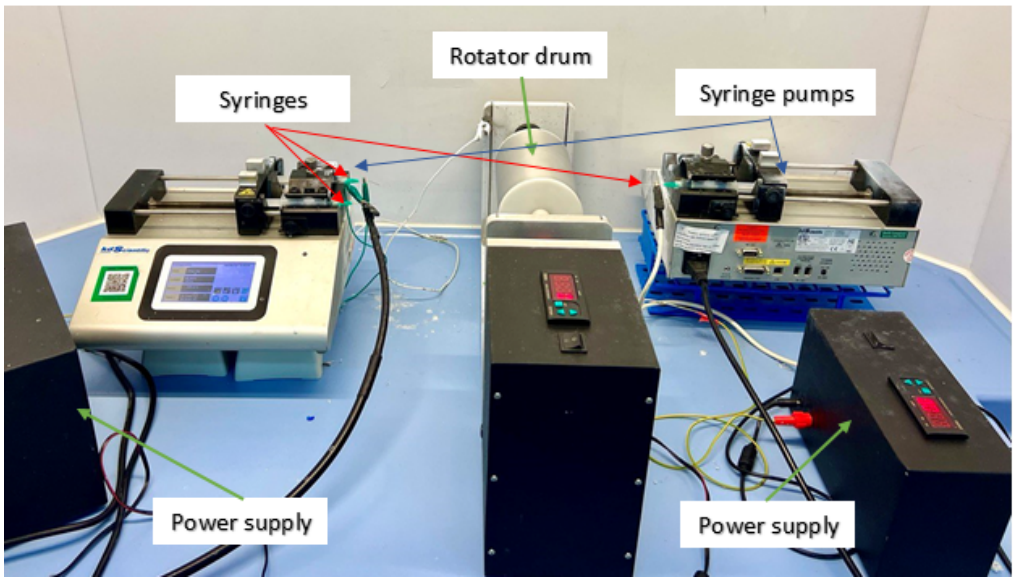

Figure 2: Setup for fabricating bimodal grafts with aligned fibers

2.3 Scanning Electron Microscope characterization of membranes

Specimens were coated with 5 nm of gold lamination (Quotrum Q150T ES, UK) and examined

using a SEM (JSM-IT200(LA), JEOL, Japan). ImageJ (National Institutes of Health, U.S.) software was utilized to assess fiber diameters. At least 100 fibers for each image were measured (n=5).

2.4 Determine diameter distribution of PET&PCL fibers

Ten vertical lines were drawn with equal spacing in the SEM images. These lines were used to determine the diameter of fibrils that crossed them. The United States National Institutes of Health's ImageJ image processing software was utilized for this measurement. To ensure accurate and statistically significant results, at least 100 fibrils per image were measured. In addition, each graft was divided into three sections, which increased the sample size and accuracy of the measurements. In each section and cohort, the diameter of fibrils crossing the reference lines was measured. For each cohort separately, the diameter distribution, mean diameter (calculated as the arithmetic average), and range (the difference between the maximum and minimum diameter) were determined. This enabled a comprehensive analysis of the diameter characteristics of fibrils in each studied cohort.

2.5 Fabrication of grafts and tensile tests

The electrospun aligned membranes were cut into pieces with 3cm width, being the dimension in the direction of fibers. Then, these membranes were rolled to make bimodal grafts with 2.0-2.5 mm in diameter and 3 cm in length as shown in Figure 3A. This method was applied for both bimodal PET&PCL and PCL grafts.

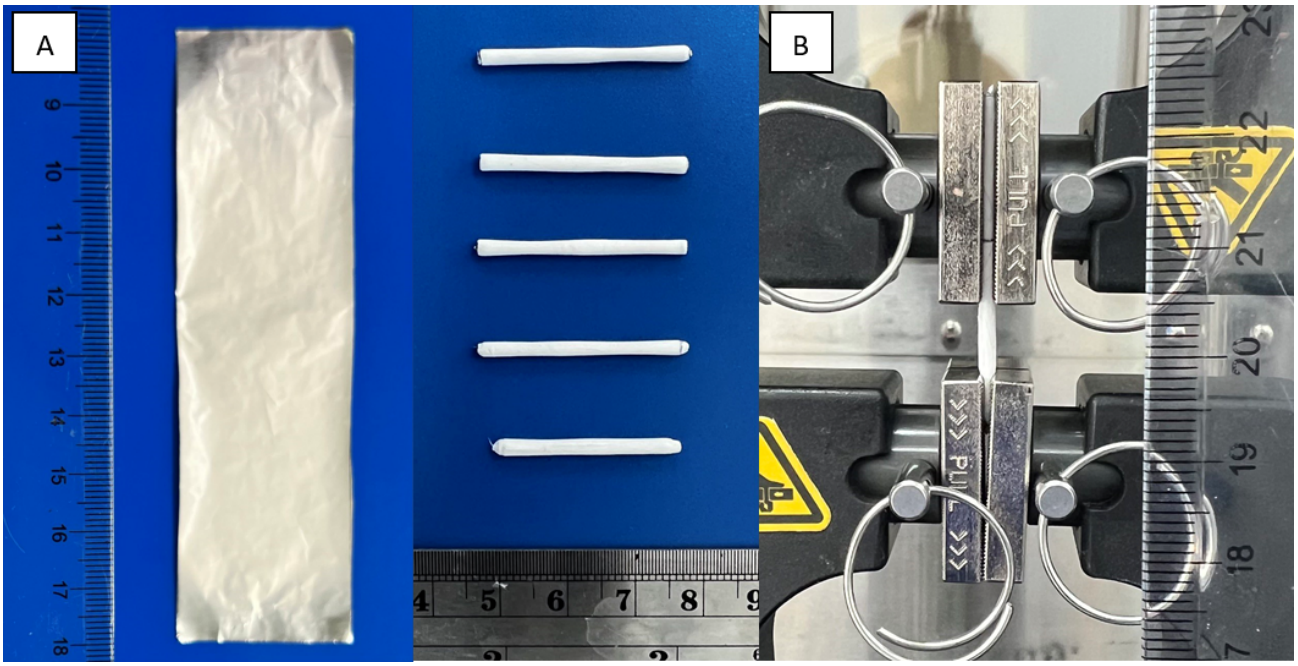

Figure 3: (A) Fabrication of grafts by rolling the electrospun membranes, (B) installation of the graft on the mechanical testing device

Using uniaxial material testing apparatus (MTS Criterion Model 43, MTS Systems Co., Eden Prairie, Minnesota, United States), the mechanical characteristics of the rolled PET&PCL and rolled PCL grafts were evaluated (Figure 3B). The dimensions of the grafts, including length, width, and thickness, were measured using a caliper, (Faithful Quality Tool, UK, Faicaldig digital caliper 150 mm). At a test speed of 5mm/min, a constant extension was applied to both PET&PCL and PCL grafts until rapture.

2.6 Testing the graft in a rabbit animal model

ACL reconstruction of the right knee using bimodal rolled graft was conducted on a four months old male rabbit weighing around 4kg. Before surgery, the rabbit was examined by a veterinarian for the presence of any diseases. The expert concluded that the animal is free of disease. Then, to anesthetize the rabbit, Xylozine (5 mg/kg) and Zoletin (0,1 mg/kg) were used. After shaving the right knee, betadine was used to clean the surface and the knee was aseptically draped. The

native ACL was excised at its femoral and tibial origins following a medial para-patellar incision and lateral patellar dislocation. At the tibia and lateral femoral condyle at the anatomical position of the native ACL 2.5 mm drill hole was created. Bimodal rolled graft was passed through the hole and ends were fixed with PGA 3/0 suture at the lateral surface of the lateral femoral condyle and medial surface of tibia. The PGA ligature helped to stabilize the knot. The incision was closed in layers. Both during and after the operation, antibiotics were administered to the animal. It was then kept in a standard cage with no restrictions in activity. Immediately after waking up, the rabbit's physical activity was monitored for 5 days. On the fifth day, the rabbit was sacrificed to get the knee joint together with the femur and tibia. The macropreparation was studied and compared with an intact knee joint with microCT analysis.

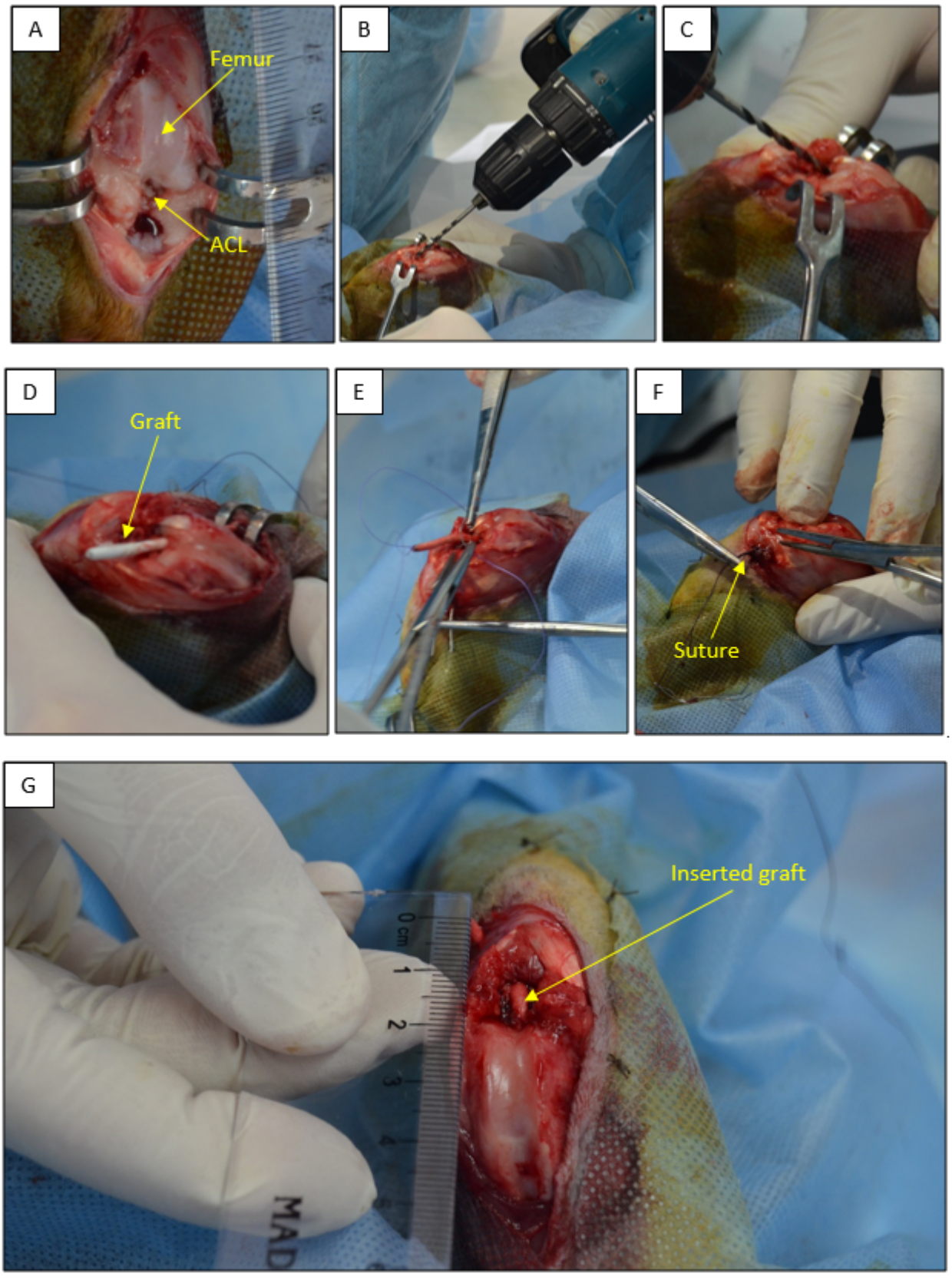
A
Femur
ACL
B
C
D
Graft
E
F
Suture
G
Inserted graft

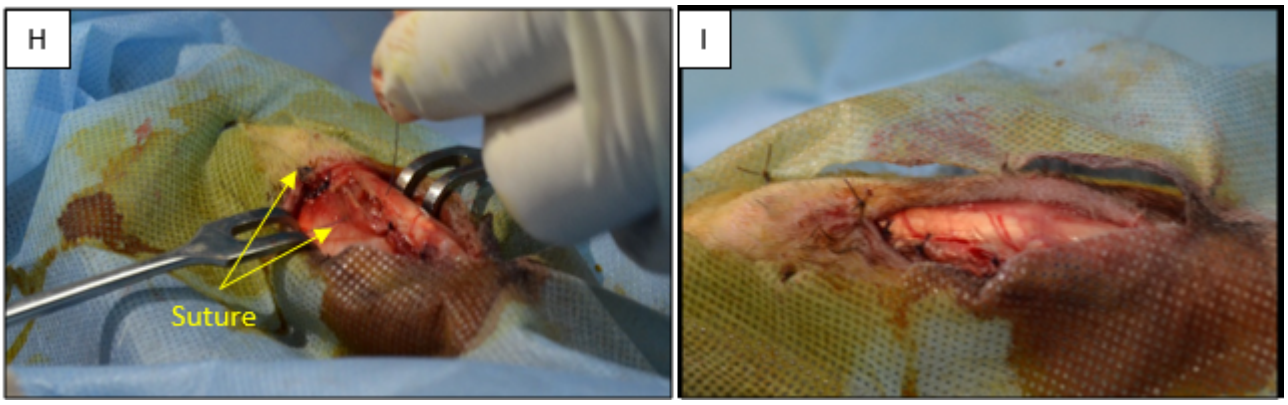

Figure 4: Photographs of the ACL replacement surgery on the rabbit. (A) the opened knee joint capsule, (B) formation of bone tunnel in femur, (C) formation of bone tunnel in tibia, (D) the proximal end of the graft passed through the femoral tunnel, (E) sutured distal end of the graft ready to pass through the tibial tunnel (F) distal end of the graft fixed in the tibial side by suturing, (G) nanofiber based rolled PET&PCL graft replaced ACL in the knee joint, (H) and (I) closing the wound by suturing layer by layer.

2.7 Micro-CT characterization

The knee joints of a rabbit were harvested and stored at 4C for 24 hours. The specimens were scanned using a μCT machine (IVIS Spectrum CT; Caliper) with the following parameters: x-ray mode with a voxel size of 150 μ, 440 Al fitter, 50 kV, a resolution of 425, and a FOV of L × W × H 12 × 12 × 13 cm, binning 4, total time 140 sec. The approximate dose per scan was 52 mGv. Using the Living Image 4.3.1 software (Caliper), the 3-D reconstruction was executed. The image was exported and preserved in the Digital Imaging and Communications in Medicine (DICOM) format.

2.8 Statistical Analysis

The mechanical properties of bimodal PET&PCL grafts, bimodal PCL grafts, and a healthy rabbit ACL were compared using a one-way analysis of variance (ANOVA) followed by the Tukey HSD (Honest Significant Difference) posthoc test. Analysis and comparison of collagen diameter of healthy ACL tissues, fiber diameter of PET&PCL construct, fiber diameter of PCL

grafts, and mechanical properties of PET&PCL and PCL grafts were conducted using an unpaired student-t test. When the p-value was less than 0.05, the difference was regarded statistically significant.

Chapter 3 – (RESULTS)

3.1 Fiber diameter of PET&PCL grafts

The histograms of the PET&PCL scaffolds are shown below in Figure 5, along with the corresponding SEM images of the scaffolds. The PET&PCL scaffolds appear to have a bimodal distribution (Fig. 5 A). Moreover, they showed a well-organized morphology, with nanofibers that were aligned in the longitudinal direction of the scaffolds (Fig. 5 B).

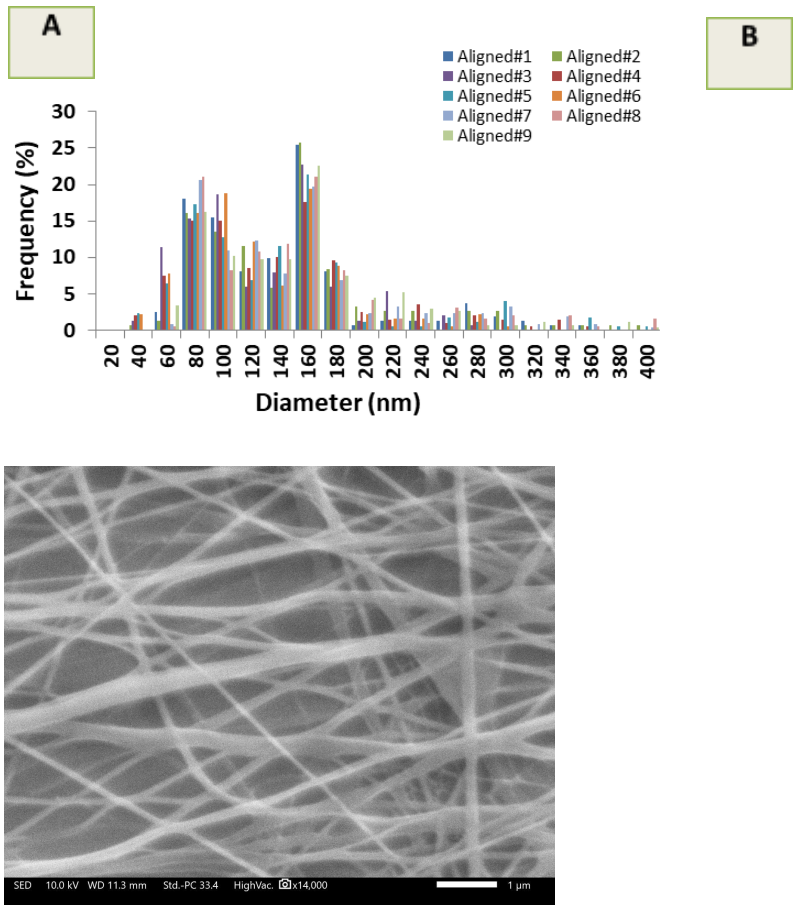

Figure 5: Diameter distribution of (A) bimodal PET&PCL fibers and (B) representative SEM images. Scale bar = 1µm.

Figure 6 shows the averaged distributions of native ACL fibrils retrieved from [28] and

PET&PCL fibers that demonstrated a bimodal (two peaks) distribution. Specifically the first peak for ACL and PET&PCL graft observed at 95±10nm and 84.4±8.8nm, respectively. The second peak was observed at 160±0.0nm for both groups. However results show that there is statistically significant difference between the diameters of native ACL fibrils and PET&PCL fibers in terms of mean diameter and number average diameter.

A

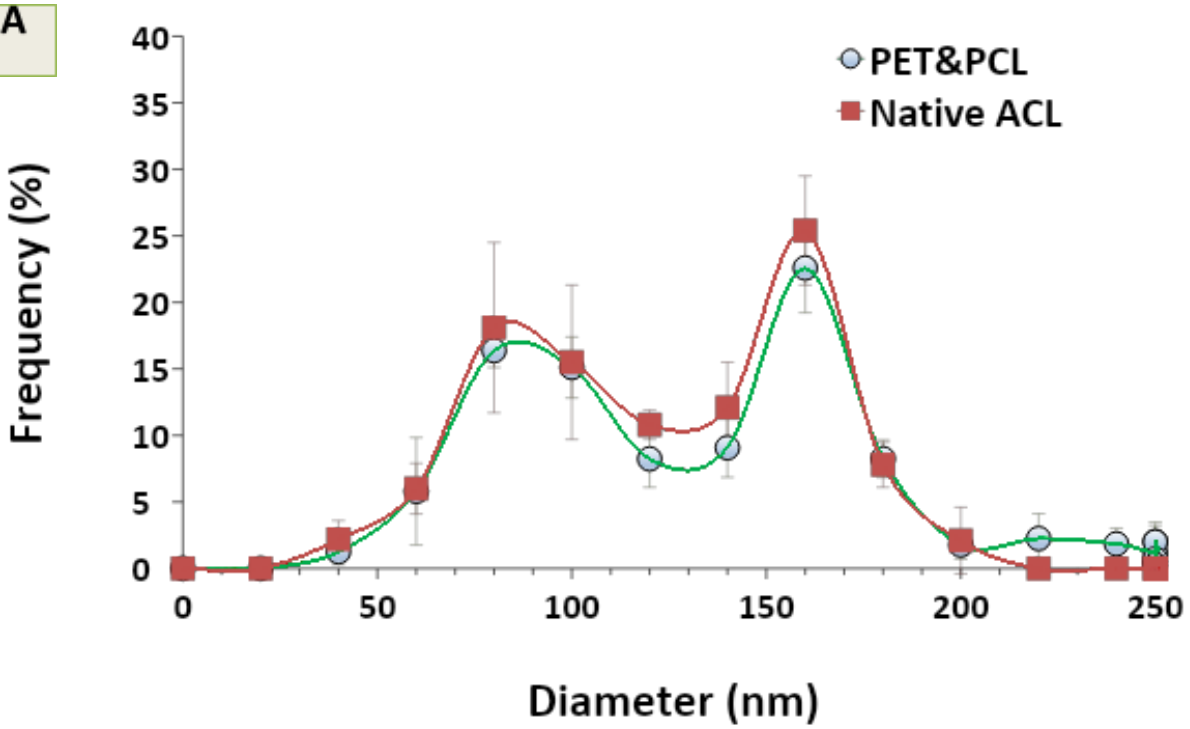

B

Fibril Diameter (nm)	PET&PCL Scaffold		Native ACL tissue	
Range	40-400		40-200	
Peak(s)	84.4±8.8	160	95±10.0	160
Mean Diameter	135±10.8*		113.5±2.4	
Number Average Diameter	143±9.2*		124.3±2.4	

* $p<0.05$

Figure 6: Comparison of diameter distribution between ACL tissue and PET&PCL grafts. (A) Healthy ACL versus Bimodal PET&PCL, and (B) descriptive statistics. Error bars denote standard deviation.

3.2 Biomechanical characteristics of PET&PCL grafts

Figure 7 depicts the load-elongation and stress-strain characteristics of native ACL tissue, PET&PCL graft and PCL-only graft. The curves begin with a toe region, which is followed by a linear region, and terminate with a yield region. All groups exhibit the characteristic of a three-phase pattern. The ultimate stress and strain in the tissue of the ACL are 27.7±6.80 N/mm^2 and 23.4±10.47 percent, respectively. This specimen's tissue modulus was calculated from the slope of the linear component of the stress - strain curve and is 1.9±0.84 MPa. The ligament's stiffness was determined to be 108.8±27.83 N/mm when it was stretched. The ACL was stretched to a load of 145.8±21.29 N with an elongation of 1.9±0.85 mm. In terms of yield region, the yield strain, yield stress and load at yield were 18.9±6.31 %, 26.1±6.09 N/mm^2 and 129.0±8.89 N, respectively.

As for the mechanical performance parameters of PET&PCL grafts, it was determined that the ultimate stress and strain of the PET&PCL grafts were 29.5±2.5 N/mm^2 and 61.7±11.8%, respectively. In the same manner, the ultimate stress and strain of the PCL grafts, which represented the negative control group, were 42.7±6.9 N/mm^2 and 140.0±2.9%, respectively. PET&PCL and PCL grafts had moduli of 1.8±0.3 MPa and 1.0±0.4 MPa, respectively. It was determined that the stiffness of PET&PCL and PCL grafts was 100.8±15.1 N/mm and 42.2±6.3 N/mm, respectively. When stretched to an ultimate elongation of 5.0±0.9 mm and 11.3±0.2 mm, the ultimate tensile load for the PET&PCL and PCL grafts was 128.3±12.2 N and 126.5±11.5 N, respectively.

Comparison of the native ACL tissue with PET&PCL and only PET grafts showed that there was no significant difference between ACL and PET&PCL in terms of maximum stress, maximum load, modulus, stiffness, yield strain and yield stress (Figure 7 C, D). On the other hand, the PCL-only grafts had significantly lower mechanical properties than ACL tissue and

PET&PCL graft in terms of stiffness (Figure 7 C, D).

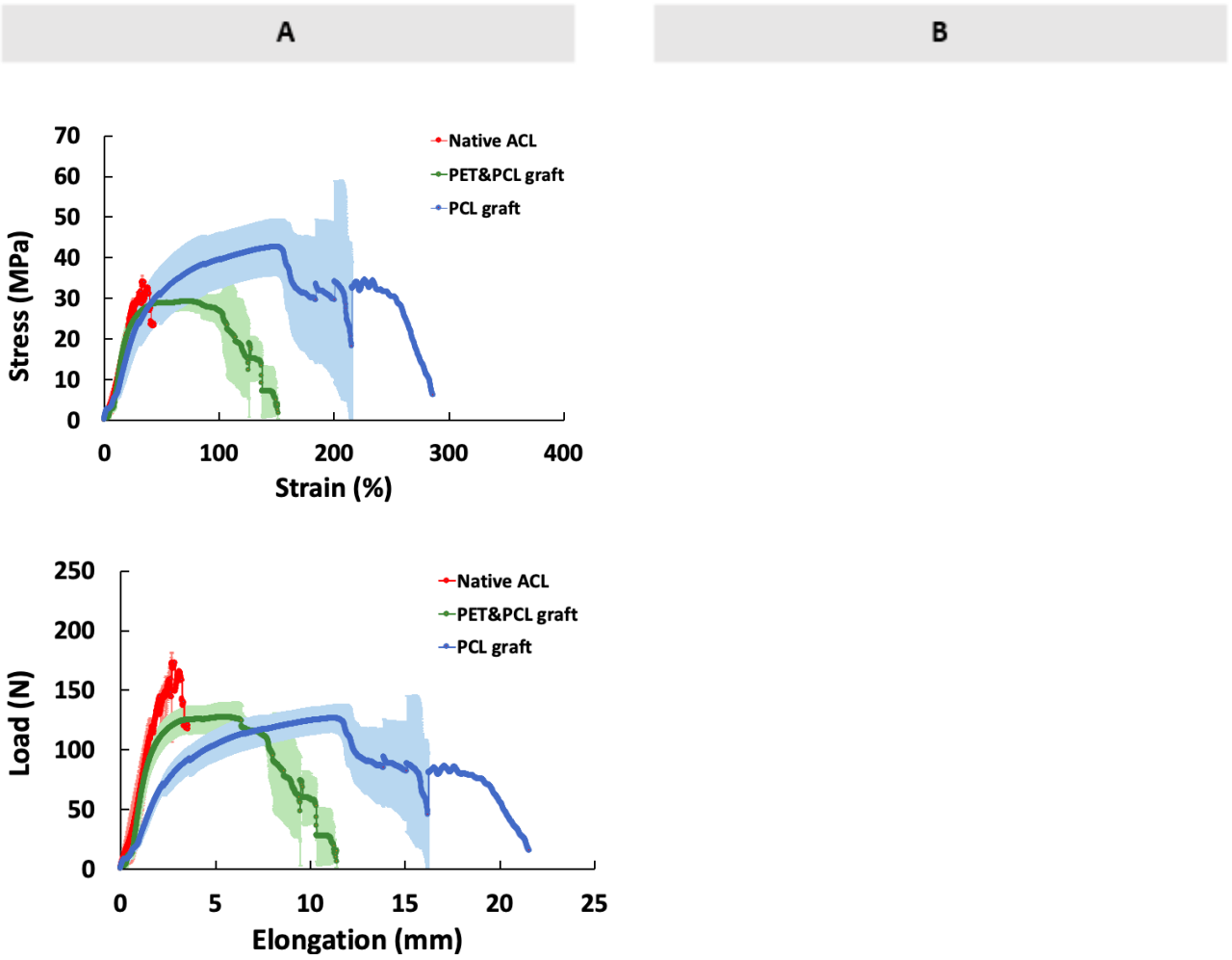

C	Ultimate Stress (N/mm^2)	Ultimate Load (N)	Ultimate Strain (mm)	Ultimate Strain (%)	Strain at Break (mm)	Strain at Break (%)	Modulus	Stiffness (N/mm)
Native ACL	27.7±6.8	145.8±21.3	1.9±0.8#*	23.4±10.5#*	2.2±1.1#*	27.0±13.9#*	1.9±0.8	108.8±27.8#
PET+PCL graft	29.5±2.5#	128.3±12.2	5.0±0.9#	61.7±11.8#	9.1±0.7	113.2±8.7	1.8±0.3	100.8±15.1#
PCL graft	42.7±6.9	126.5±11.5	11.3±0.2	140.0±2.9	13.4±2.7	166.9±33.8	1.0±0.4	4.2±6.3

D	Yield Strain (%)	Yield Stress (N/mm^2)	Yield Load (N)
Native ACL	18.9±6.31	26.1±6.09	129.0±8.89#*
PET+PCL	17.8±1.9	18.4±0.7	75.1±4.3#
PCL	21.6±3.9	16.9±1.9	56.5±7.8

Figure 7: Comparison of Native ACL tissue, PET&PCL grafts, and PCL grafts in terms of mechanical properties. (A) Stress-strain diagram, (B) Load-elongation diagram, (C) and (D)

descriptive statistics. An * indicates significant difference from PET&PCL graft and # indicates significant difference from PCL graft at p<0.05. Error bars represent SD.

3.3 Evaluation of implants after ACL reconstruction in a rabbit model

Gross view of the PET&PCL grafts (Figure 8A) was similar to the native ACL (Figure 8B). However, our previous PCL-only graft (Figure 8C) deformed permanently and was unable to stabilize the knee joint after implantation.

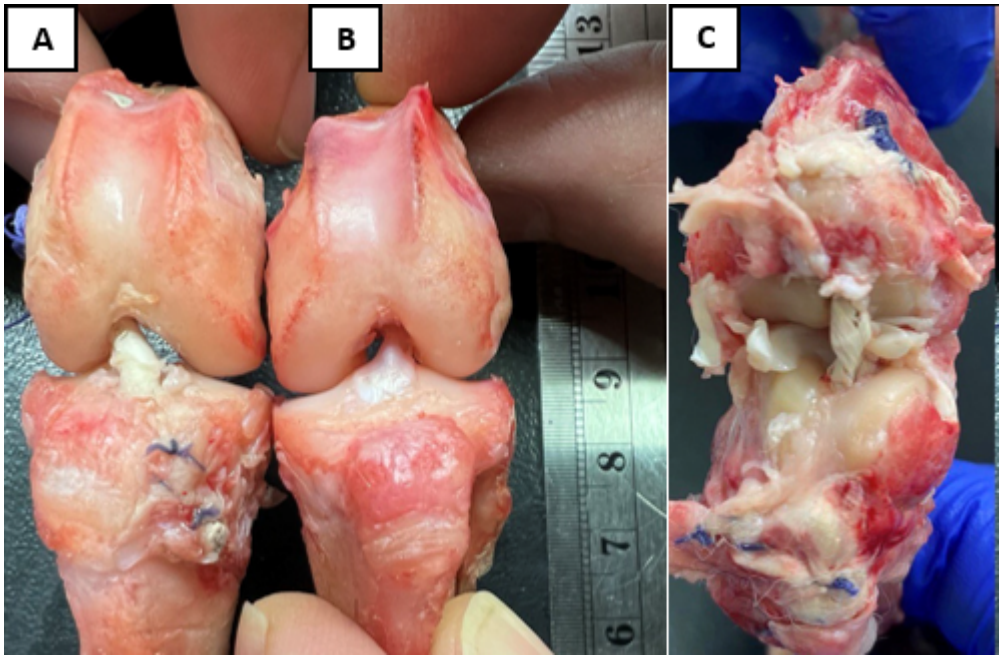

Figure 8: Gross view of the knee joints harvested from rabbits at Day5. (A) After ACL reconstruction with rolled bimodal PET&PCL graft, (B) intact knee joint (native ACL), (C) after ACL reconstruction with braided bimodal PCL-only graft.

3.4 MicroCT evaluation of bone tunnels

MicroCT images of the rabbit knee joints harvested at Day 5 clearly demonstrate presence of bone tunnel drilled for ACL reconstruction. Apparently, no bone is formed within the tunnel during the short period of reconstruction (Figure 9).

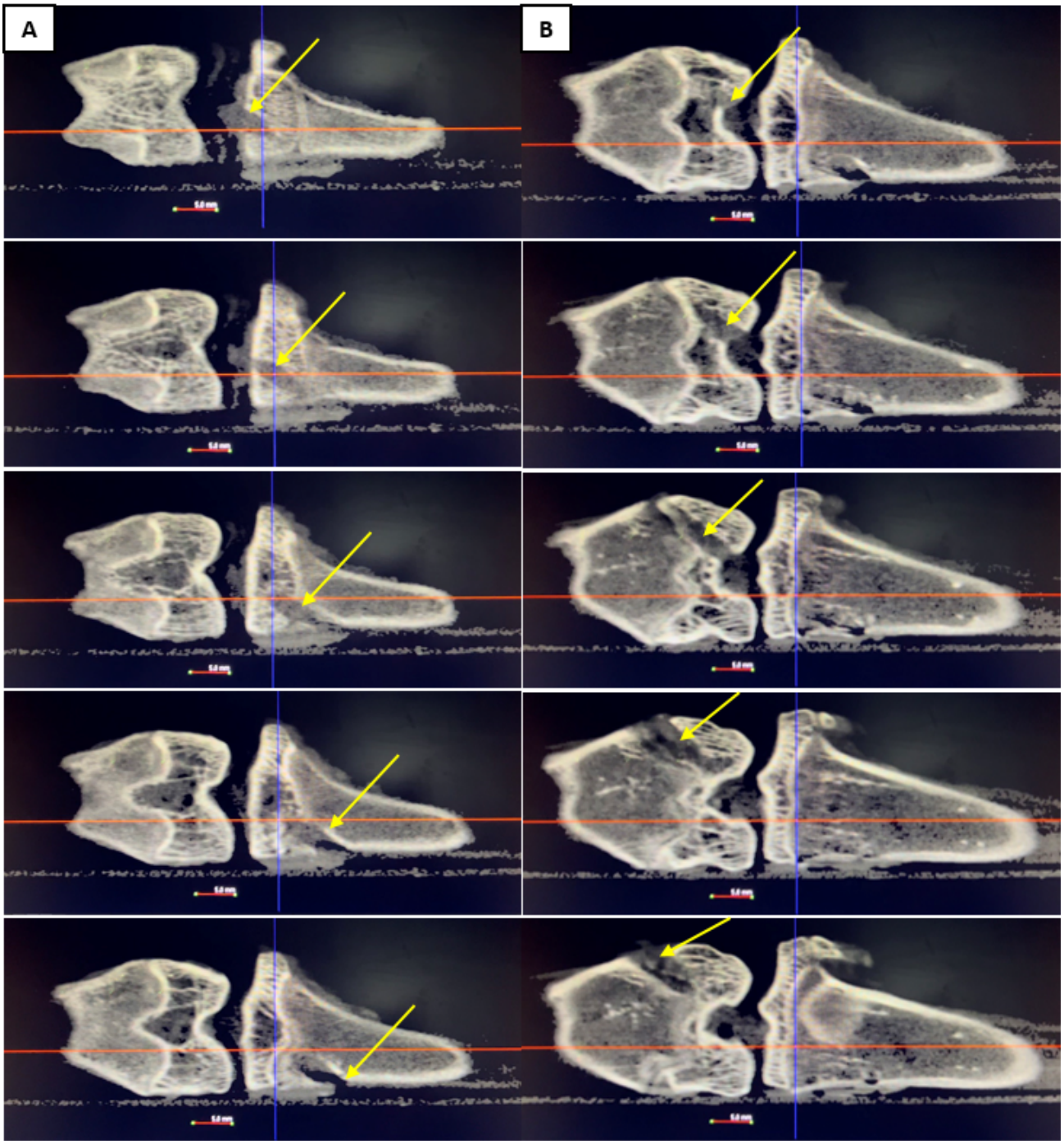

Figure 9: MicroCT images of the rabbit's knee joint after ACL replacement with bimodal PET&PCL graft (A) Bone tunnel in tibia (B) Bone tunnel in femur. Scale bar =5mm

CHAPTER 4 - (DISCUSSION)

In this study, a nanofiber-based PET&PCL graft for rabbit ACL reconstruction was created to mimic the microstructure of the native ligament. It is common knowledge that ligaments, including the ACL, have a hierarchical structure and are composed of collagen fibers of various diameters. For example, in the human anterior cruciate ligament (ACL), the smallest subfibrils have a diameter of 40 to 140 nm and form fibrils with a diameter of 150 to 840 nm [23]. Some authors argue that the composition of the ACL can change with age. However, research on young people has revealed that the majority of this ligament is composed of collagen fibrils ranging in size from 20 to 180 nm [24]. Studies conducted on animals have also confirmed that the ACL is composed of nanoscale collagen fibers [25], [26], [27]. Our team's previous research on rabbits revealed that the diameter of ACL collagen fibers ranges from 40 to 200 nm [28] while the results of our current study indicate that the nanofibers from PET and PCL have diameters ranging from 40 to 400 nm. However, there is a significant difference between the mean diameters of the native ACL (113.5±2.4 nm) and the graft (135±10.8 nm); and the number average diameters of the native tissue (124.3±2.4 nm) and the PET&PCL graft (143±9.2 nm). It is primarily due to the PET portion's origin of fibrils with larger diameters. In this study, the lowest concentration of PET was used based on the spinnability properties of this polymer, as stated in [29], and other electrospinning process parameters were modified to produce nanofibers that resembled native tissue collagen fibers. Because it is well known that the remodeling of tissue fiber microgeometry plays a role in the efficacy of ligament reconstructive treatments [23].

As numerous studies have demonstrated a correlation between the diameter distribution of collagen fibers and the mechanical properties of the ligament [30], bimodal distribution results in greater tensile properties, whereas unimodal distribution is predominantly observed in injured

ligament tissues and is associated with biomechanical weaknesses [31]. Processing SEM images by diameter size reveals a bimodal distribution of PET&PCL nanofibers, with two peaks at 84.4±8.8 nm and 160nm. According to [28], the rabbit's native ACL has a bimodal organization of fibers with the first peak at 95±10.0 nm and the second peak at 160nm. Similarly, previous studies on other animals demonstrated a bimodal pattern of fibers: bovine, ovine, and rat had two peaks at 73 and 213 nm, 100 and 250 nm, and 60 and 160 nm, respectively, and all showed unimodal distribution after injury [25], [26], [27]. This indicates that our bimodal PET&PCL grafts completely mimic the native ACL tissue's behavior in terms of structure, and that the bimodal composition would improve its' mechanical ability, thereby preventing ruptures.

Bimodal distribution results in improved mechanical properties because the smaller fibers fill the space between the larger fibers, making the structure dense. Incorporating PET, which possesses superior mechanical properties [15], increased the bimodal graft's tensile strength even further. Therefore, there are no differences between the native ACL and both types of bimodal grafts in terms of maximum stress, maximum load, modulus, yield strain and yield stress. However, in terms of stiffness, PET&PCL demonstrated comparable results to native ACL while PCL grafts demonstrated significantly lower results. Stiffness for PET&PCL grafts was 100.8±15.1 N/mm, whereas this figure for PCL grafts was 42.2±6.3 N/mm. Even though PET&PCL have greater elongation than a native ACL, consisting of 5.0±0.9 mm and 1.9±0.85 mm, respectively, this figure is considerably lower than that of PCL, which is 11.3±0.2 mm. Both PET&PCL and PCL grafts performed worse than native ACL in terms of strain at break parameter. This could be related to the overall polymer characteristics during the tensile test. Nevertheless, this bimodal PET&PCL graft is able to stabilize the knee joint due to its similar modulus and stiffness to native ACL tissue as well as its lower elongation than PCL grafts.

After rabbit ACL reconstruction surgery, the bimodal rolled PET&PCL graft stabilized the knee joint, whereas the PCL braided graft elongated. In both instances, the animal's physical activity was not restricted, and results were obtained five days after surgery. There was no difference in

length between the PET&PCL grafts before and after 5 days of activity, whereas the PCL graft almost doubled in length.

MicroCT analysis is a technique for assessing the formation of new bone [32] as well as the tunnel enlargement for various reasons, one of which may be a mechanical factor [33] and the drilling technique. The MicroCT analysis performed 5 days after surgery to evaluate the bone tunnels created in the femur and tibia on the ACL insertion sides revealed no difference. Possible causes include the shorter duration of the study and the smaller diameter of the needle used to drill the bone tunnel. As some authors [34] have suggested that larger bone tunnels may be advantageous for bone formation.

CHAPTER 5 - (CONCLUSION)

The aim of this research was to investigate the structural and functional characteristics of a graft fabricated from PET&PCL, and compare it with the native rabbit ACL. The results revealed that the graft exhibited similarities with the native tissue in terms of both diameter distribution and mechanical properties. This finding is significant as it indicates that the PET&PCL graft could be a suitable synthetic graft for ACL reconstruction.

This study is original because it is the first study to propose a method for the fabrication of a PET&PCL graft with bimodal distribution for ACL reconstruction. Therefore, the findings of this research will have promising implications for the advancement of orthopedic research and clinical practice.

Further studies involving in vitro and in vivo experiments on rabbit models will be conducted to evaluate the performance and biocompatibility of the PET&PCL graft.

REFERENCE LIST

[1] M. Marieswaran, I. Jain, B. Garg, V. Sharma, and D. Kalyanasundaram, "A Review on Biomechanics of Anterior Cruciate Ligament and Materials for Reconstruction," *Applied Bionics and Biomechanics*, vol. 2018, pp. 1–14, 2018, doi: https://doi.org/10.1155/2018/4657824.

[2] B. P. Boden, G. S. Dean, J. A. Feagin, Jr, and W. E. Garrett, Jr, "Mechanisms of Anterior Cruciate Ligament Injury," *Orthopedics*, vol. 23, no. 6, pp. 573–578, Jun. 2000, doi: https://doi.org/10.3928/0147-7447-20000601-15.

[3] T. L. Sanders *et al.*, "Incidence of Anterior Cruciate Ligament Tears and Reconstruction: A 21-Year Population-Based Study," *The American journal of sports medicine*, vol. 44, no. 6, pp. 1502–7, 2016, doi: https://doi.org/10.1177/0363546516629944.

[4] L. S. Lohmander, P. M. Englund, L. L. Dahl, and E. M. Roos, "The Long-term Consequence of Anterior Cruciate Ligament and Meniscus Injuries," *The American Journal of Sports Medicine*, vol. 35, no. 10, pp. 1756–1769, Oct. 2007, doi: https://doi.org/10.1177/0363546507307396.

[5] T. Piontek *et al.*, "Arthroscopically Assisted Combined Anterior and Posterior Cruciate Ligament Reconstruction with Autologous Hamstring Grafts–Isokinetic Assessment with Control Group," *PLoS ONE*, vol. 8, no. 12, p. e82462, Dec. 2013, doi: https://doi.org/10.1371/journal.pone.0082462.

[6] N. A. Friel and C. R. Chu, "The Role of ACL Injury in the Development of Posttraumatic Knee Osteoarthritis," *Clinics in Sports Medicine*, vol. 32, no. 1, pp. 1–12, Jan. 2013, doi: https://doi.org/10.1016/j.csm.2012.08.017.

[7] D. Little, J. W. Thompson, L. G. Dubois, D. S. Ruch, M. A. Moseley, and F. Guilak, "Proteomic Differences between Male and Female Anterior Cruciate Ligament and Patellar Tendon," *PLoS ONE*, vol. 9, no. 5, pp. 1–14, May 2014, doi: https://doi.org/10.1371/journal.pone.0096526

[8] B. R. Bach, M. E. Levy, J. Bojchuk, S. Tradonsky, C. A. Bush-Joseph, and N. H. Khan, "Single-Incision Endoscopic Anterior Cruciate Ligament Reconstruction Using Patellar Tendon Autograft," *The American Journal of Sports Medicine*, vol. 26, no. 1, pp. 30–40, Jan. 1998, doi: https://doi.org/10.1177/03635465980260012201.

[9] P. Zhang, F. Han, T. Chen, Z. Wu, and S. Chen, "'Swiss roll'-like bioactive hybrid scaffolds for promoting bone tissue ingrowth and tendon-bone healing after anterior cruciate ligament reconstruction," *Biomaterials Science*, vol. 8, no. 3, pp. 871–883, 2020, doi: https://doi.org/10.1039/c9bm01703h.

[10] E. Bayrak, B. Ozcan, and C. Erisken, "Processing of polycaprolactone and hydroxyapatite to fabricate graded electrospun composites for tendon-bone interface regeneration," *Journal of Polymer Engineering*, vol. 37, no. 1, pp. 99–106, Jan. 2017, doi: https://doi.org/10.1515/polyeng-2016-0017.

[11] M.-O. Christen and F. Vercesi, "Polycaprolactone: How a Well-Known and Futuristic Polymer Has Become an Innovative Collagen-Stimulator in Esthetics," *Clinical, Cosmetic*

and Investigational Dermatology, vol. Volume 13, pp. 31–48, Jan. 2020, doi: https://doi.org/10.2147/ccid.s229054.

[12] M. A. Woodruff and D. W. Hutmacher, "The return of a forgotten polymer—Polycaprolactone in the 21st century," *Progress in Polymer Science*, vol. 35, no. 10, pp. 1217–1256, Oct. 2010, doi: https://doi.org/10.1016/j.progpolymsci.2010.04.002.

[13] R. M. Mohamed and K. Yusoh, "A Review on the Recent Research of Polycaprolactone (PCL)," *Advanced Materials Research*, vol. 1134, pp. 249–255, Dec. 2015, doi: https://doi.org/10.4028/www.scientific.net/amr.1134.249.

[14] Dalton P D, Woodfield T, and Hutmacher D W, "SnapShot: Polymer Scaff olds for Tissue Engineering," *Biomaterials*, vol. 30, no. 4, pp. 701–702, Feb. 2009, doi: https://doi.org/10.1016/s0142-9612(08)00900-9.

[15] N. J. Rowden, D. Sher, G. J. Rogers, and K. Schindhelm, "Anterior Cruciate Ligament Graft Fixation," *The American Journal of Sports Medicine*, vol. 25, no. 4, pp. 472–478, Jul. 1997, doi: https://doi.org/10.1177/036354659702500409.

[16] B. Li, Y. Wen, H. Wu, Q. Qian, Y. Wu, and X. Lin, "Arthroscopic single-bundle posterior cruciate ligament reconstruction: retrospective review of hamstring tendon graft versus LARS artificial ligament," *International Orthopaedics*, vol. 33, no. 4, pp. 991–996, Jul. 2008, doi: https://doi.org/10.1007/s00264-008-0628-6.

[17] A. P. Rumian, A. L. Wallace, and H. L. Birch, "Tendons and ligaments are anatomically distinct but overlap in molecular and morphological features—a comparative study in an ovine model," *Journal of Orthopaedic Research*, vol. 25, no. 4, pp. 458–464, 2007, doi: https://doi.org/10.1002/jor.20218.

[18] S. Jafari, S. S. Hosseini Salekdeh, A. Solouk, and M. Yousefzadeh, "Electrospun polyethylene terephthalate (PET) nanofibrous conduit for biomedical application," *Polymers for Advanced Technologies*, vol. 31, no. 2, pp. 284–296, Nov. 2019, doi: https://doi.org/10.1002/pat.4768.

[19] J. D. Schiffman and C. L. Schauer, "A Review: Electrospinning of Biopolymer Nanofibers and their Applications," *Polymer Reviews*, vol. 48, no. 2, pp. 317–352, May 2008, doi: https://doi.org/10.1080/15583720802022182.

[20] M. Bachy, I. Sherifi, F. Zadegan, D. Petrover, H. Petite, and D. Hannouche, "Anterior cruciate ligament surgery in the rabbit," *Journal of Orthopaedic Surgery and Research*, vol. 8, no. 1, Aug. 2013, doi: https://doi.org/10.1186/1749-799x-8-27.

[21] B. L. Proffen, M. McElfresh, B. C. Fleming, and M. M. Murray, "A comparative anatomical study of the human knee and six animal species," *The Knee*, vol. 19, no. 4, pp. 493–499, Aug. 2012, doi: https://doi.org/10.1016/j.knee.2011.07.005.

[22] A. L. Bascuñán, A. Biedrzycki, S. A. Banks, D. D. Lewis, and S. E. Kim, "Large Animal Models for Anterior Cruciate Ligament Research," *Frontiers in Veterinary Science*, vol. 6, Aug. 2019, doi: https://doi.org/10.3389/fvets.2019.00292.

[23] L.-H. . Yahia and G. Drouin, "Collagen structure in human anterior cruciate ligament and patellar tendon," *Journal of Materials Science*, vol. 23, no. 10, pp. 3750–3755, Oct. 1988, doi: https://doi.org/10.1007/bf00540523.

[24] R. Strocchi, P. V. De, A. Facchini, M. Raspanti, S. Zaffagnini, and M. Marcacci, "Age-related changes in human anterior cruciate ligament (ACL) collagen fibrils," *Italian*

journal of anatomy and embryology = Archivio italiano di anatomia ed embriologia, vol. 101, no. 4, pp. 213–220, Oct. 1996, Accessed: Apr. 10, 2023. [Online]. Available: https://europepmc.org/article/med/9203869

[25] Z. Beisbayeva, A. Zhanbassynova, G. Kulzhanova, F. Mukasheva, and C. Erisken, "Change in Collagen Fibril Diameter Distribution of Bovine Anterior Cruciate Ligament upon Injury Can Be Mimicked in a Nanostructured Scaffold," *Molecules*, vol. 26, no. 5, p. 1204, Jan. 2021, doi: https://doi.org/10.3390/molecules26051204.

[26] S. Smatov, "Polycaprolactone based nanofiber scaffolds can mimic collagen fibril diameter distribution of healthy and injured sheep Anterior Cruciate Ligament," Nazarbayev University, Astana, KZ, 2021.

[27] A. O. Adeoye *et al.*, "A biomimetic synthetic nanofiber-based model for anterior cruciate ligament regeneration," *Front. Bioeng. Biotechnol.*, vol. 10, p. 969282, 2022.

[28] S. Kadyr, "Synthetic Polycaprolactone grafts for Anterior Cruciate Ligament," Nazarbayev University, Astana, KZ, 2022.

[29] A. Hadjizadeh, A. Ajji, and M. N. Bureau, "Nano/micro electro-spun polyethylene terephthalate fibrous mat preparation and characterization," *Journal of the Mechanical Behavior of Biomedical Materials*, vol. 4, no. 3, pp. 340–351, Apr. 2011, doi: https://doi.org/10.1016/j.jmbbm.2010.10.014.

[30] C. Niyibizi, K. Kavalkovich, T. Yamaji, and S. L-Y. Woo, "Type V collagen is increased during rabbit medial collateral ligament healing," *Knee Surgery, Sports Traumatology, Arthroscopy*, vol. 8, no. 5, pp. 281–285, Aug. 2000, doi: https://doi.org/10.1007/s001670000134.

[31] K. Shino, B. W. Oakes, S. Horibe, K. Nakata, and N. Nakamura, "Collagen Fibril Populations in Human Anterior Cruciate Ligament Allografts," *The American Journal of Sports Medicine*, vol. 23, no. 2, pp. 203–209, Mar. 1995, doi: https://doi.org/10.1177/036354659502300213.

[32] P. P. Y. Lui *et al.*, "Inferior tendon graft to bone tunnel healing at the tibia compared to that at the femur after anterior cruciate ligament reconstruction," *Journal of Orthopaedic Science*, vol. 15, no. 3, pp. 389–401, May 2010, doi: https://doi.org/10.1007/s00776-010-1460-6.

[33] J. Höher, H. D. Möller, and F. H. Fu, "Bone tunnel enlargement after anterior cruciate ligament reconstruction: fact or fiction?," *Knee Surgery, Sports Traumatology, Arthroscopy*, vol. 6, no. 4, pp. 231–240, Oct. 1998, doi: https://doi.org/10.1007/s001670050105.

[34] H. Yu *et al.*, "Biomechanical, histologic, and molecular characteristics of graft-tunnel healing in a murine modified ACL reconstruction model," *Journal of Orthopaedic Translation*, vol. 24, pp. 103–111, Jun. 2020, doi: https://doi.org/10.1016/j.jot.2020.05.004.